

A Tight-Binding Investigation of the Na_xCoO_2 Fermi Surface

M. D. JOHANNES, D. A. PAPACONSTANTOPOULOS, D. J. SINGH, M. J. MEHL
Code 6391, Naval Research Laboratory, Washington, D.C. 20375

PACS. 71.20.-b – Electron density of states and band structure of crystalline solids.
 PACS. 71.18.+y – Fermi surface: calculations and measurements, effective mass, g-factor.

Abstract. – We perform an orthogonal basis tight binding fit to an LAPW calculation of paramagnetic Na_xCoO_2 for several dopings. The optimal position of the apical oxygen at each doping is resolved, revealing a non-trivial dependence of the band structure and Fermi surface on oxygen height. We find that the small e_g' hole pockets are preserved throughout all investigated dopings and discuss some possible reasons for the lack of experimental evidence for these Fermi sheets.

The compound Na_xCoO_2 has been synthesized for a wide range of Na contents, $0.3 < x < 0.9$, and exhibits a variety of unusual phenomena that are strongly dependent on doping level. Study of $\text{Na}_{0.5}\text{CoO}_2$ for its surprisingly good thermoelectric properties began several years ago [1] and more recently, attention has been focused on the hydrated compound $\text{Na}_{0.35}\text{CoO}_2 \cdot 1.3\text{H}_2\text{O}$ which undergoes a superconducting phase transition at $T \sim 4.5\text{K}$ [2,3].

The behavior and characteristics of Na_xCoO_2 do not vary smoothly along the spectrum of Na contents, but instead split very generally into two separate metallic phases separated at $x=0.5$ by an insulating phase [4]. The low Na content region at $x < 0.5$ is characterized by conventional metallic behavior [5] and a nearly temperature independent susceptibility [6,8] indicating a Pauli paramagnetic precursor to the superconducting state. The linear specific heat coefficient γ is measured to be $\sim 12\text{-}16 \frac{\text{mJ}}{\text{molK}^2}$ which shows only light mass renormalization [6,7]. In contrast, the high Na region at $x > 0.5$, though also metallic, exhibits a Curie-Weiss-like susceptibility [9,10,12]. A higher (compared to the previous metallic phase) measured γ of $25\text{-}30 \frac{\text{mJ}}{\text{molK}^2}$ indicates that mass renormalization in this region is substantial [9,12,15]. Interestingly, the Kadawaki-Woods ratio, a comparison of γ to the quadratic coefficient of resistivity, which is often used as a measure of electron-electron interaction, is reported to be the largest ever measured and considerably field dependent [16]. This may evidence a nearby quantum critical point and indeed, μsR and transport measurements show a magnetic transition in single crystals at $T=22\text{K}$ for dopings of $x=0.7$ and $x=0.75$, usually interpreted as a spin density wave [10,13,14]. Strong ferromagnetic spin fluctuations have been predicted based on LDA calculations [11] and have been detected by neutron scattering [17] when $x=0.7$, but with slightly higher electron count at $x=0.85$, a bulk anti-ferromagnetic transition has been reported [18], suggesting the presence of more than one type of magnetic interaction. The insulating phase is very narrowly centered at $x=0.5$ and recent reports show both charge and

magnetic order [4], though earlier investigations, most notably work by Terasaki et al [1,19,20], found this system to be metallic. Measurements of $\gamma \sim 40\text{--}56 \frac{\text{mJ}}{\text{molK}^2}$ are higher than for any other doping [19,20] and NMR measurements indicate Curie-Weiss behavior and charge separation [21].

Here we present a highly accurate tight-binding parameterization of Na_xCoO_2 , obtained for a range of apical oxygen heights at each of three dopings: $x=0.3, 0.5$, and 0.7 , meant to be representative of the three general phases. We anticipate that this Hamiltonian will be valuable as accurate, material-specific input to model systems that can incorporate the important effects of correlation. We point out that, since the system is multi-band in nature, a strictly two-dimensional triangular lattice model is insufficient to fully account for all dispersions. In contrast to earlier tight-binding models [22,23], we include both interlayer couplings and all five Co- d orbitals as a basis. The nearly perfect reproduction of LDA Fermi level crossings within our tight-binding scheme allows a detailed and accurate examination of doping and structural Fermi surface dependencies. We show that the band structure is strongly coupled to the apical oxygen height which itself depends on the amount of charge donated to the CoO_2 plane by Na ions. A rigid band picture is insufficient to describe the evolution from small x where the band structure is nearly two dimensional to large x where non-negligible interplanar coupling causes heavy distortion of one Fermi sheet. An important effect of increased three-dimensionality in the high Na compounds is the preservation of the small hole pockets at the K points of the Brillouin zone (BZ). We discuss possible reasons that these pockets are absent from ARPES measurements [28,29].

Through a series of calculations with an LAPW implementation (Wien2k) [24] of DFT formalism, we varied the Na level, x , of Na_xCoO_2 , holding the total volume constant at 509.553 a.u.^3 . Though important effects may derive from the specific location of Na ions, particularly in the insulating compound at $x=0.5$, where Na and charge order are thought to cooperate, we treat Na in the virtual crystal approximation (VCA) and concentrate only on effects stemming directly from variation of electron number. Specifically, we treat every Na site as fully occupied, but with a fictitious ion of atomic charge $10.x$, rather than a true Na atom of charge 11. This approximation is most valid when the Na states are far from the Fermi energy, as they are Na_xCoO_2 for all x , and in fact, comparison of VCA and Na ordered calculations show little difference [25]. The apical oxygen height was relaxed for a number of dopings and shown to increase non-linearly with Na addition. The optimal O position as a fraction of the lattice constant ($a=5.366824 \text{ a.u.}$) for $x=0.3, 0.5$ and 0.7 was found to be $0.0811, 0.0834$, and 0.0864 respectively. The six Co-derived bands near the Fermi energy in each of these first-principles calculations form the basis for our tight-binding fit.

We fit the LAPW eigenvalues using the NRL tight-binding method [27]. Assuming that the important features of the band structure are due to Co and O ion interactions, we used a basis set consisting of 5 Co- d orbitals for each of two Co sites and 3 O- p orbitals for each of four O sites resulting in 25 Slater Koster (SK) hopping parameters and 5 on-site energies to vary. The six bands ($4 e_g$ and $2 a_{1g}$) nearest the Fermi energy are cleanly separated from the e_g bands above and O $2p$ bands below by an energy gap [26] allowing them to be isolated from all other bands during the fit by a weighting of the eigenvalues. The orthogonality of our basis set was enforced and site symmetry taken into account by requiring that on-site energies of orbitals in a given irreducible representation be the same. We kept neighbors up to a distance greater than half the c -axis lattice parameter to account for inter-planar coupling. Because this basis set and number of neighbors results in a large amount of freedom, the parameters that fit the LAPW band structure accurately are not unique, and several solutions which nicely reproduced the calculated dispersions were found. In order to distinguish the desired physically relevant solution (*i.e.* atomic-like orbital picture), we compared the tight-binding

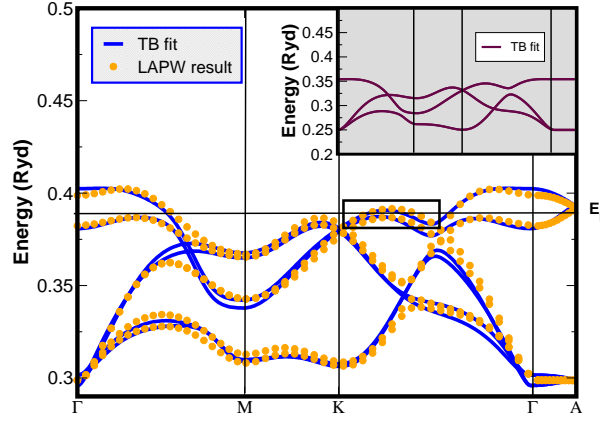


Fig. 1 – A tight-binding fit to the $\delta = 0.7$ optimal apical oxygen height band structure. The rectangular box indicates the Fermi level crossing responsible for the $e_{g'}$ elliptical hole pockets. The upper inset has an expanded c-axis to eliminate inter-planar coupling.

eigenvectors to the orbitally resolved LAPW band structure at each k-point. The criteria that the characters of each eigenvalue must qualitatively match was used to identify a single set of parameters as the correct one.

For each doping, we fit to band structures with three different apical O heights: one above, one below and one at the optimal position. Since the NRL-TB parameters are expressed as polynomials in distance, we could fit all O positions at each doping simultaneously, thereby explicitly including O height dependence in the parameterization. The familiar SK elements are then easily obtained for any structure by evaluating the NRL-TB parameters at a specific distance. A table of SK elements and on-site energies for all three dopings is provided in Tables I and II, with the O position set at its relaxed height in each case. A typical fit (that of $x=0.7$) is shown in fig. 1. The Fermi level crossings are reproduced almost exactly, though there are small discrepancies in dispersion lower in energy, most notably between Γ and M. The rectangular box highlights the $e_{g'}$ band as it breaks above the Fermi energy; this feature is responsible for the small hole Fermi sheets which will be the central concern of this paper.

The TB fit yields relative positions of the on-site energy parameters for the Co-d orbitals as expected from simple symmetry considerations: the xy, x^2-y^2 orbitals are highest in energy, the xz, yz orbitals sit lowest and the $3z^2-r^2$ (or a_{1g}) orbital is raised slightly above the latter. Similarly, the in-plane O onsite energies, p_x and p_y , are higher than the out-of-plane energy, p_z . It is important to note that the orbitals familiarly designated as $e_{g'}$ and e_g are both combinations of the xz, yz and xy, x^2-y^2 representations in the hexagonal coordinate system. On a simple triangular lattice (that of the Co ions alone), these representations do not mix, but the distorted octahedra of O ions breaks local z-reflection symmetry and facilitates hoppings that would otherwise be forbidden, *i.e.* Co-Co hopping between orbitals that are ostensibly orthogonal takes place through O ions positioned non-symmetrically above and below the Co plane. A combination of all characters ($3z^2-r^2$, xz, yz , and xy, x^2-y^2) is present anywhere that a_{1g} and $e_{g'}$ bands mix. At the very top of the band complex, mostly above the Fermi energy, the character is purely a_{1g} , but elsewhere throughout the energy region $e_{g'}$ character is also present. Both band types cross the Fermi level, necessitating a multi-band treatment for accurate reproduction of the DOS and Fermi surfaces. At the very least, any model meant to reproduce both a_{1g} and $e_{g'}$ bands on a triangular lattice must include all five Co d-orbitals,

TABLE I – *Hopping Integrals (meV)*

		Co-O		O-O		Co-Co		
		$dp\sigma$	$dp\pi$	$pp\sigma$	$pp\pi$	$dd\sigma$	$dd\pi$	$dd\delta$
d=0.3	1st n.n.	-1286	1054	112	30	-326	34	34
	2nd n.n.	-33	21	78	228	2	72	-68
	3rd n.n.	0	-8	56	132	0	13	-62
	4th n.n.			53	122			
	5th n.n.			18	30			
d=0.5	1st n.n.	-1422	1003	250	20	-405	63	36
	2nd n.n.	-53	33	135	198	33	63	-83
	3rd n.n.	-2	-3	107	133	4	11	-57
	4th n.n.			100	115			
	5th n.n.			44	27			
d=0.7	1st n.n.	-1551	929	295	59	-433	90	16
	2nd n.n.	-88	64	309	187	52	56	-97
	3rd n.n.	-4	-9	204	156	6	10	-47
	4th n.n.			167	119			
	5th n.n.			55	17			

TABLE II – *On-site Energies (eV)*

	$x=0.3$	$x=0.5$	$x=0.7$
xy, x^2-y^2	3.578	4.204	4.762
xz, yz	2.422	3.184	3.850
z^2	2.558	3.360	4.122
p_x, p_y	0.272	0.653	1.116
p_z	-0.830	0.0	0.735

and the symmetry breaking property of the O ions further implies that even this will not necessarily account for all dispersions.

We now discuss the main doping and related structural dependencies of the band dispersions. In the VCA, the addition of Na narrows the overall bandwidth of what would be, in an ideal octahedral environment, the t_{2g} complex. The insensitivity of this bandwidth to c-axis compression suggests that extra charge shifts the balance between competing in-plane interactions, thus decreasing dispersion. Hoppings perpendicular to the plane break the degeneracy of the two layers and cause an important splitting of the a_{1g} bands near the Γ point, but have relatively little effect elsewhere. If inter-layer hopping is eliminated by, for example, a pronounced expansion of the c-axis length, the six bands collapse onto three doubly degenerate bands and the splitting disappears (see inset of fig. 1). Not surprisingly, inter-layer coupling increases with growing Na content until at $x=0.7$, the two a_{1g} bands are separated by as much as 20% of the total t_{2g} bandwidth along the Γ -A line. The final, and in terms of this discussion most important, effect of Na charge is its determination of the apical O height which in turn establishes the magnitude of the e_g - a_{1g} split. Coulomb repulsion in the Co-O plane shifts the apical O position upward, easing the octahedral distortion and lowering the a_{1g} band weight center relative to e_g . Additional charge mainly enters the lowered a_{1g} band, leaving the e_g hole pockets intact, though diminished in size. The cumulative result of these effects is summarized in fig. 2 where the varying bandwidths and inter-planar splittings corresponding

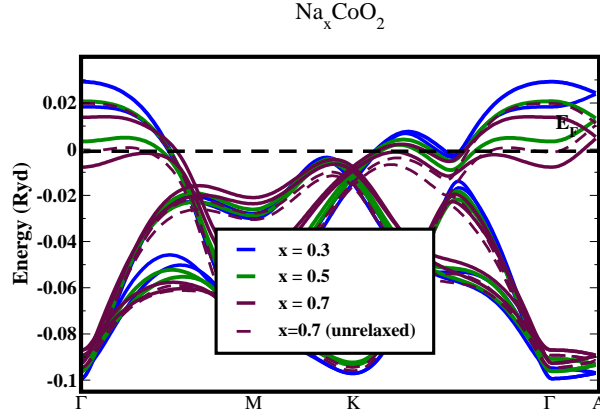


Fig. 2 – The bandstructures of Na_xCoO_2 for three values of x , plotted with Fermi energies aligned. The $x=0.7$ calculation is performed at both relaxed and unrelaxed O positions; in the latter the e_g' hole surface disappears.

to each Na level are shown. A second calculation of the $x=0.7$ compound, but with the apical O at an unrelaxed height (we chose the $x=0.3$ height for comparison) illustrates the effect of apical O re-positioning. At the unrelaxed (lower) height, only a_{1g} bands cross the Fermi level and e_g' states are completely filled, eliminating the small pockets from the Fermi surface.

We calculated the Fermi surfaces for each doping using our TB parameters and a very dense mesh of nearly 8000 \vec{k} -points in the BZ. Generating the eigenvalues at each of these points in the tight-binding scheme requires less than 1/1000th the amount of computing time that an LAPW code uses for the same task. For each doping, there is a doubly degenerate a_{1g} -like hexagonal large hole pocket at the top of the BZ, and six doubly degenerate small hole pockets near K which are e_g' -like (see fig. 3). Moving toward the zone center, the two surfaces disperse away from each other, one surface growing and the other shrinking. In the $x=0.3$ case, the dispersion is small for both surfaces, and the system is essentially two-dimensional. For the $x=0.5$ doping, the dispersion is stronger, particularly that of the inner or shrinking surface which becomes somewhat hourglass shaped. At $x=0.7$, the z -dispersion of the inner surface is so strong that it splits into two separate sheets, disappearing entirely at the zone center. The outer surface, in contrast, remains fairly dispersionless. Both surfaces for this doping are shown in fig. 3. The increase in z -dispersion with electron number is due to both the upward shift of the O ions as more charge is dumped into the Co-O plane and to increased hybridization effects of the charge itself. When Na is added, holes come mainly out of the shrinking inner surfaces, mainly the hexagonal one and to a lesser degree the elliptical ones, with the effect that the e_g' hole sheets are robust with respect to doping in the outer surface and are preserved, though barely, in the inner surface.

Recent photoemission experiments [28,29] have clearly seen a large Fermi surface consistent with the a_{1g} derived section predicted in LDA calculations. The small primarily e_g' derived pockets were not seen. This could be due to surface sensitivity of these states, for example, due to a different surface potential related to surface Na stoichiometry, which would shift the positions of these bands or to a relaxation of the O height in the top layer, which would also shift these bands. As we have demonstrated, the apical O must be a certain distance from the Co plane for e_g' Fermi sheets to exist at the $x=0.7$ doping. Therefore, contraction of the Co-O complex at the surface may indeed serve to depress the e_g' feature responsible

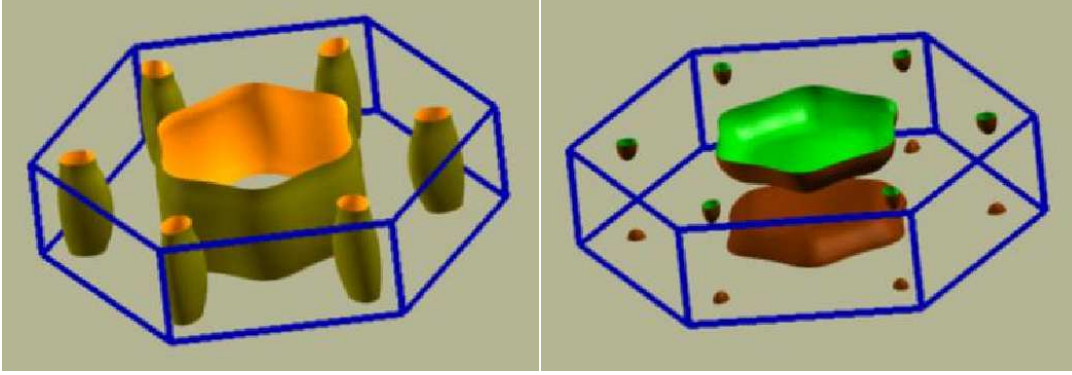


Fig. 3 – The outer (left) and inner (right) Fermi sheet of $\text{Na}_{0.7}\text{CoO}_2$. The increased charge present in the Co-O planes both raises the apical oxygen position and increases hybridization, making the z-dispersion non-negligible. The inner surface shows 3-d dispersion in large (a_{1g}) and small ($e_{g'}$) hole pockets

for the small hole pockets as exemplified by the unrelaxed calculation of $\text{Na}_{0.7}\text{CoO}_2$ in fig. 2. Alternatively, it may be that correlation effects neglected by the LDA change the position of the $e_{g'}$ band and eliminate the small pockets at dopings where ARPES measurements have been made, namely at $x=0.65$ and $x=0.7$. K.-W. Lee *et al* have suggested, based partly on the same experimental evidence that prompted division of the phase diagram into three sections, that non-negligible static correlation exists only in the high Na region [30]. It is possible to produce a relative shift of the a_g and e'_g derived bands in our tight binding analysis by shifting the corresponding on-site parameters for $x > 0.5$. This mimics what would happen in a non-spin-polarized LDA+U calculation [31] where the tendency toward integer occupation of orbitals strongly disfavors small Fermi surfaces such as the $e_{g'}$ pockets. We caution that while LDA+U band shifts have been used *e.g.* in Ni to improve the agreement between calculated and experimental Fermi surfaces [32], the physics of applying a static mean field correlation like LDA+U to a metallic system can be questioned [33], as it is known that fluctuation effects as in the dynamical mean field theory (DMFT) are very important. A 0.067 Ry shift of the a_{1g} onsite parameter (corresponding to a Hubbard U of 3 eV) eliminates the small ellipses from the $x=0.7$ Fermi surface and enlarges the hexagonal pocket slightly to accommodate the lost holes. If these hole pockets are indeed missing due to correlation effects, then the bandstructure can successfully be modelled with a single band (a_{1g}) and the distinction between triangular and pseudo-hexagonal structures discussed previously becomes unimportant.

In conclusion, we have constructed a tight-binding Hamiltonian which can accurately reproduce the LDA Fermi surfaces and band dispersions of Na_xCoO_2 for $x=0.3, 0.5$ and 0.7 . Relaxation of the apical oxygen position at each doping reveals that the Fermi surface is non-trivially dependent on doping level and that holes preferentially enter and leave from the larger a_{1g} -like surface, preserving the smaller hole pockets as charge is added. Foo *et al* [5] observed three rather distinct regions in the phase space of x , two magnetic and one insulating. Our calculations show that the system passes from quasi-two-dimensionality at low Na content to anisotropic three-dimensionality at high Na content. This may have bearing on the very different magnetic and thermodynamic properties observed on either side of the insulating phase boundary, though the insulating state itself is not reproduced by the LDA. We address the differences in predicted and observed Fermi surfaces and postulate that either

surface distortion or possibly correlation could account for the discrepancies.

* * *

We would like to thank C. S. Hellberg, M. Z. Hasan, S. Nagler, D. Mandrus and I. Terasaki for contributing useful perspective and discussions. We are particularly indebted to I. I. Mazin for his insights into symmetry properties and their ramifications. M.D.J is supported by a National Research Council associateship. Research at NRL is funded by the Office of Naval Research.

REFERENCES

- [1] TERASAKI I., SASAGO Y. and UCHINOKURA K., *Phys. Rev. B*, **56** (1997) 12685.
- [2] TAKADA K., SAKURAI H., TAKAYAMA-MUROMACHI E., IZUMI F., DILANIAN R. A. and SASAKI R., *Nature*, **422** (2003) 53
- [3] SCHAAK R. E., KLIMCZUK T., FOO M. L. and CAVA R. J., *Nature*, **424** (2003) 527
- [4] HUANG Q., FOO M. L., LYNN J. W., ZANDBERGEN H. W., LAWES G., WANG Y., TOBY B. H., RAMIREZ A. P., ONG N. P. and CAVA R. J., *cond-mat/0402255*, (2004)
- [5] FOO M. L., WANG Y., WATUCHI S., ZANDVERGEN H. W., HE T., CAVA R. J. and ONG N. P., *Phys. Rev. Lett.*, **92** (2004) 247001
- [6] JIN R., SALES B. C., KHALIFAH P. and MANDRUS D., *Phys. Rev. Lett.*, **91** (2003) 217001
- [7] UELAND B. G., SCHIFFER P., SCHAAK R. E., FOO M. L., MILLER V. L., and CAVA R. J., *Physica C*, **402** (2004) 27
- [8] CHOU F. C., CHO J. H., LEE P. A., ABEL E. T., MATAN K. and LEE Y. S., *Phys. Rev. Lett.*, **92** (2004) 157004
- [9] SUGIYAMA J., BREWER H., ANSALDO J., ITAHARA H., TANI T., MIKAMI M., MORI Y., SASAKI T., HEVERT S. and MAIGNAN A., *J. Phys. Cond. Mat.*, **15** (2003) 8619
- [10] SALES B. C., JIN R., AFFHOLTER K. A., KHALIFAH P., VEITH G. M. and MANDRUS D., *cond-mat/0402379*, (2004)
- [11] SINGH D. J., *Phys. Rev. B*, **68** (2003) 020503
- [12] MOTOHASHI T., UEDA R., NAUJALIS E., TOJO R., TERASAKI I., ATAKE T., KARPPINEN M. and YAMAUCHI H., *Phys. Rev. B*, **67** (2003) 064406
- [13] SUGIYAMA J., ITAHARA H., BREWER J. H., ANSALDO E. J., MOTOHASHI T., KARPPINEN M., and YAMAUCHI H., *Phys. Rev. B*, **67** (2003) 214420
- [14] PRABHAKARAN D., BOOTHROYD A. T., CODEA R., HELME L. M., and TENNANT D. A., *cond-mat/0312493*, (2003)
- [15] BRUHWILER M., BATLOGG B., KAZAKOV S. M. and KARPINSKI J., *cond-mat/0309311*, (2003)
- [16] LI S. Y., TAILLEFER L., HAWTHORN D. G., TANATAR M. A., PAGLIONE J., SUTHERLAND M., HILL R. W., WANT C. H. and CHEN X. H., *Phys. Rev. Lett.*, **93** (2004) 056401
- [17] BOOTHROYD A. T., COLDEA R., TENNANT D. A., PRABHAKARAN D. and FROST C. D., *Phys. Rev. Lett.*, **92** (2004) 197201
- [18] BAYRAKCI S., BERNHARD C., CHEN D. P., KEIMER B. and KREMER R. K., *Phys. Rev. B*, **69** (2004) 100410
- [19] ANDO Y., MIYAMOTO N., SEGAWA K., KAWATA T. and TERASAKI I., *Phys. Rev. B*, **60** (1999) 10580
- [20] TERASAKI I., *Physica B*, **328** (2003) 63
- [21] RAY R., GHOSHRAY A. and GHOSHRAY K., *Phys. Rev. B*, **59** (1999) 9454
- [22] KOSHIBAE W., and MAEKAWA S., *Phys. Rev. Lett.*, **91** (2003) 257003
- [23] KUMAR B., and SHASTRY B. S., *Phys. Rev. B*, **68** (2003) 104508
- [24] BLAHA P., SCHWARZ K., MADSEN G. K. H., KVASNICKA D. and LUITZ J.,
An Augmented Plane Wave + Local Orbitals Program for Calculating Crystal Properties (Karlheinz Schwarz, Techn. Universitat Wien, Austria), ISBN 3-9501031-1-2

- [25] JOHANNES M. D., SINGH D. J., *Phys. Rev. B*, **70** (2004) 014507
- [26] SINGH D. J., *Phys. Rev. B*, **61** (2000) 13397
- [27] PAPACONSTANTOPOULOS D. A., MEHL M. J., *J. Phys. Condens. Matter*, **15** (2003) R413
- [28] HASAN M. Z., CHUANG Y. -D., KUPRIN A., KONG Y., QIAN D., LI Y. W., MESLER B., HUSSAIN Z., FEDOROV A. V., KIMMERLING R., ROTENBERG E., ROSSNAGEL K., KOH H., ROGADO N. S., FOO M. L. and CAVA R. J., *Phys. Rev. Lett*, **92** (2004) 246402
- [29] YANG H. -B., WANG S. -C., SEKCHARAN A. K. P., MATSUI H., SOUMA S., SATO T., TAKAHASHI T., TAKEUCHI T., CAMPUZANO J. C., JIN R., SALES B. C., MANDRUS D., WANG Z. and DING H., *Phys. Rev. Lett.*, **92** (2004) 246403
- [30] LEE K. -W., KUNES J. and PICKETT W. E., *Phys. Rev. B*, **70** (2004) 045104
- [31] PAPACONSTANTOPOULOS D. A. and HELLBERG C. S., *Phys. Rev. Lett.*, **89** (2002) 029701
- [32] YANG I., SAVRASOV S. Y. and KOTLIAR G., *Phys. Rev. Lett*, **87** (2001) 216405
- [33] PETUKHOV A. G., MAZIN I. I., CHIONCEL L. and LICHTENSTEIN A. I., *Phys. Rev. B*, **67** (2003) 153106